Differentiating Subtle Variation of Weak Intramolecular Hydrogen Bond in Vicinal Diols by Linear Infrared Spectroscopy

Xiaoyan Ma and Jianping Wang*

Beijing National Laboratory for Molecular Sciences, State Key Laboratory of Molecular Reaction Dynamics, Institute of Chemistry, Chinese Academy of Sciences, Beijing 100190, P. R. China
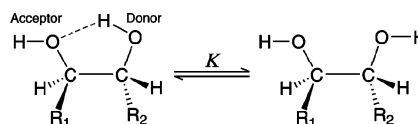
Received: February 21, 2009

Linear IR spectra show "free" and intramolecular hydrogen-bonded (IHB) −OH groups in vicinal diols as two separate O−H stretching absorption bands. Here we present a case study of four linear vicinal diols with different alkyl groups: 1,2-ethylene glycol, 1,2-propanediol, 2,3-butanediol, and 1,2-butanediol. By carefully removing contributions from anharmonic vibrational coupling and local structural effect, "pure" IHB-resulted frequency separation and peak enhancement are obtained and found to exhibit a linear relationship between them. The results suggest that the IHB formation energy in the diols is structurally dependent, and 1,2-propanediol has the smallest vibrational contribution to the IHB energy among the four diols examined.

Introduction

By participating in inter- or intramolecular hydrogen bonds (H-bonds), the hydroxyl group (−OH) plays an important role in stabilizing molecular complexes ranging from acids, phenols, alcohols, and sugars, to peptides and DNA bases.[1−7] However, the characterization of the −OH-group-containing H-bond, in particular, the weak intramolecular hydrogen bond (IHB), still remains a challenge for experimentalists.[6] A five-membered quasiring structure (Scheme 1, left) containing two OH groups in vicinal diols presents a very intriguing case of such weak IHB. In fact, because of unfavorable HB-forming geometry associated with a semirigid structure, the existence of IHB has been debated for quite some time. Nuclear magnetic resonance (NMR),[8] vibrational circular dichroism,[9] and infrared (IR) experiments[10−14] clearly show evidences of IHB presented in various diols,[15,16] which is supported by theoretical computations,[17−19] even though recent electron density topology computations[20−22] seem to suggest the opposite. For such IHB structure in diols, questions arise as to whether the HB strength varies from structure to structure and whether it is possible to quantify the subtle differences of the HB strength experimentally.

It is well-known that for an OH group, participating in a HB usually means a red shift in its fundamental IR stretching frequency accompanied by an increased absorption cross section, showing that vibrational spectroscopy such as linear IR can be used as a sensitive tool for examining HB complexes. On the basis of the IR absorption frequency shift ($\Delta\nu$) between free (−O−H) and H-bonded (−O−H···X) groups, empirical relationships between $\Delta\nu$ and the enthalpy, ΔH, of H-bond formation were proposed a long time ago by Badger and Bauer (B−B equation)[23,24] on the basis of a number of acids and alcohols and by Iogansen (Iogansen equations).[25] These equations have been used, for example, to estimate H-bond interaction energy in various cases.[14,21,26,27] However, for the case of vicinal diols, "free" OH and intramolecularly H-bonded OH groups shown in Scheme 1 have very close stretching frequencies. Therefore, it is difficult to determine the enthalpy

* Corresponding author. Tel: (+86)-010-62656806. Fax: (+86)-010-62563167. E-mail: jwang@iccas.ac.cn.

SCHEME 1: Vicinal Diol Equilibrium in Condensed Phase[a]

[a] R$_1$ and R$_2$ can be H, CH$_3$, or C$_2$H$_5$. H-bond acceptor and donor are labeled on the two OH groups on the left side.

experimentally. No empirical relationship between enthalpy and frequency shift has been reported for diols either.

For the vicinal diols, the observed vibrational frequency shift between "free" and H-bonded OH stretches depends not only on H-bonding conditions but also on anharmonic vibrational coupling (VC) and on chemical environment (CE) effects, meaning the following is probably true

$$\Delta\nu = \Delta\nu_{HB} + \Delta\nu_{VC} + \Delta\nu_{CE} \qquad (1)$$

However, separating these contributions, in many cases, is not straightforward. Equation 1 suggests that $\Delta\nu_{HB}$ should be the "pure" frequency shift due to HB formation, provided that it could be properly assessed.

Here we present a case study of a selection of four linear vicinal alkyl diols with different alkyl groups (Figure 1 inserts): 1,2-ethylene glycol (1,2-EG), (±)-1,2-propanediol (1,2-PD), (2R,3R)-2,3-butanediol (2,3-BD), and (±)-1,2-butanediol (1,2-BD). We carried out a linear IR (FTIR) experiment in combination with quantum chemical computations and vibrational excitonic Hamiltonian modeling. We show that some terms in eq 1 can be determined from the linear IR experiment, and some can be evaluated by the computations and modelings. Using the obtained $\Delta\nu_{HB}$ as a measure, we determine the vibrational stabilization contribution to the enthalpy of the IHB formation for the four vicinal diols. We also manage to obtain the equilibrium constant between H-bonded and free OH species, from which the total enthalpy is estimated. In combination with the enthalpies evaluated from empirical equations, we show that the strength of the weak IHB in vicinal diols is structurally dependent and its vibrational stabilization energy is smaller in structurally asymmetric diols than in symmetric ones.

Subtle Variation of Weak IHB in Vicinal Diols

J. Phys. Chem. A, Vol. 113, No. 21, 2009 **6071**
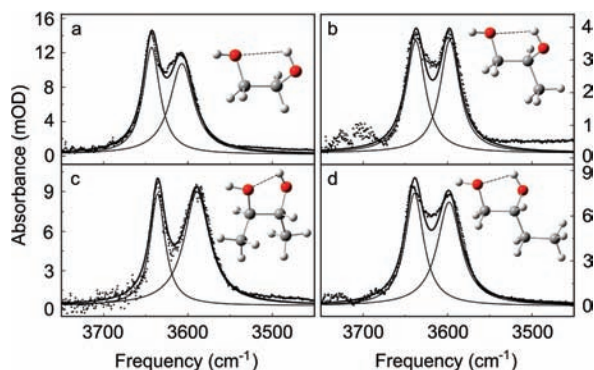
Figure 1. Linear IR spectra in the OH stretching region and molecular structures (inserts) of the four diols in CCl₄: (a) 1,2-EG, 1.8 mM; (b) 1,2-PD, 0.9 mM; (c) 2,3-BD, 1.2 mM; (d) 1,2-BD, 1.1 mM. Fitting uses Lorentzian function. Noisy signal near 3700 cm⁻¹ is due to residual water in sample. Sample temperature: 23 °C.
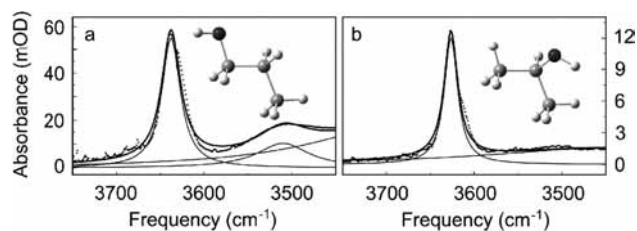
Experimental Section

Materials. Analytical reagent grade 1,2-ethylene glycol (1,2-EG), (±)-1,2-propanediol (1,2-PD), 1-propanol, and 2-propanol (purity ≥95%) were obtained from Beijing Chemical (China). Commercial (2R,3R)-2,3-butanediol (2,3-BD, purity ≥98%) was purchased from Johnson Matthey (England). (±)-1,2-butanediol (1,2-BD, purity ≥98%) was purchased from Acros (Belgium). All chemicals were used without further purification.

Linear Infrared Measurement. FTIR spectra with frequency ranging from 4000 to 1000 cm⁻¹ were collected using a Nicolet 6700 spectrometer (Thermo Electron) with a spectral resolution of 1 cm⁻¹ and were averaged for 64 scans. A CaF₂ IR sample cell with a 950 μm path length was used. All diol samples were dissolved in carbon tetrachloride (CCl₄) with concentrations of 1.8 (1,2-EG), 0.9 (1,2-PD), 1.2 (2,3-BD), and 1.1 mM (1,2-BD). A low concentration was used to ensure monodispersed solute molecules. At least three FTIR measurements for each sample were performed at room temperature (23 °C) for statistical analysis. FTIR spectra of the diols were also recorded at higher temperatures (40, 60, and 80 °C) using a homemade thermal bath. Sample temperature was directly monitored on the IR cell. FTIR spectra of the two monohydric alcohols in CCl₄ were also measured at room temperature under the following conditions: 1-propanol (169.9 mM, 250 μm IR cell spacer) and 2-propanol (38.6 mM, 100 μm spacer). IR absorption bands in the OH stretching region in each case were fitted with Lorentzian functions.

Computational Methods

Geometry optimization and normal-mode frequency calculation of the four chosen diols, 1,2-EG, 1,2-PD, 2,3-BD, and 1,2-BD, were carried out at the level of B3LYP/6-31+G*. This combination of theory and basis sets is believed to be useful in predicting gas-phase vibrational frequencies of midsized biomolecules.[28] Geometries of the four diols were fully optimized

with tight convergence criteria. No imaginary frequency was observed in their normal-mode frequencies, indicating that the optimized structures were at their global minima on the potential energy surfaces. The natural population analysis (NPA)[29] was performed at the same level of theory to examine the H-bond-induced charge redistributions of various groups. The natural bond orbital (NBO) computation was performed to evaluate changes in hyperconjugation upon the formation of an IHB complex. All computations were carried out using Gaussian 03.[30]

Figure 2. FTIR spectra in the OH stretching region for propanols in CCl₄: (a) 1-propanol, (b) 2-propanol. Molecular structures are also shown. Sample temperature: 23 °C.

Results and Discussion

Linear Infrared Spectra. Linear IR spectra of the four diols in the OH stretching region at low concentration in CCl₄ are given in Figure 1: (a) 1,2-EG, (b) 1,2-PD, (c) 2,3-BD, and (d) 1,2-BD. Molecular structures shown in the Figure 1 inserts are their lowest energy gas-phase conformers. Substantial differences in IR peak separation and intensity are clearly observed. The high-frequency band arises from the free OH group, whereas the low-frequency band can be attributed to H-bonded OH. The values of ν, $\nu_{1/2}$ (full width at half-maximum, fwhm), $\Delta\nu$, and R (= S_{intra}/S_{free}, ratio of integrated peak area), are listed in Table 1 with root-mean-square analysis. Immediately, one sees that 2,3-BD has the largest $\Delta\nu$ and R values, implying the strongest IHB. However, the value of $\Delta\nu$ does not correlate well with that of R in the four cases. In particular, one sees that 1,2-PD has a relatively larger $\Delta\nu$ but the smallest R among the four cases, suggesting that $\Delta\nu$ and R may have somewhat different origins.

Origin of Frequency Shift. To understand the origin of $\Delta\nu$, we first examine the CE effect proposed in eq 1. Local structure difference of the two OH groups may cause nondegeneracy in their fundamental transition frequencies ($\Delta\nu_{CE} \neq 0$). However, because of structure symmetry, $\Delta\nu_{CE}$ is expected to be very small for 1,2-EG and 2,3-BD because two OH groups presumably have a very similar chemical environment when they are not H-bonded. For structurally asymmetric diols, monohydric alcohols can be used to evaluate $\Delta\nu_{CE}$. Figure 2 shows FTIR spectra of 1-propanol and 2-propanol in CCl₄ in the OH stretching region. The component near 3500 cm⁻¹ is considered to be H-bonded clusters. The more-or-less concentration-independent free OH stretch vibrational frequency of 1-propanol is 3637.6 cm⁻¹, and that of 2-propanol is 3626.5 cm⁻¹. Their

TABLE 1: Frequency (ν, cm⁻¹), Full Width at Half-Maximum ($\nu_{1/2}$, cm⁻¹), Frequency Shift ($\Delta\nu$, cm⁻¹), and Integrated Peak Area Ratio ($R = S_{intra}/S_{free}$) of the Two OH Absorption Bands for the Four Diols

	OH$_{free}$		OH$_{intra}$			
species	ν	$\nu_{1/2}$	ν	$\nu_{1/2}$	$\Delta\nu$	R
1,2-EG	3642.8 ± 0.2	24.4 ± 0.2	3607.2 ± 0.2	34.1 ± 0.2	35.6 ± 0.4	1.18 ± 0.04
1,2-PD	3637.3 ± 0.5	27.4 ± 0.2	3597.4 ± 0.6	28.0 ± 0.2	39.9 ± 1.1	1.01 ± 0.04
2,3-BD	3635.5 ± 0.4	21.7 ± 0.2	3589.6 ± 0.4	36.9 ± 0.2	45.9 ± 0.8	1.79 ± 0.06
1,2-BD	3639.2 ± 0.2	26.7 ± 0.2	3597.7 ± 0.2	35.5 ± 0.6	41.5 ± 0.4	1.16 ± 0.04

TABLE 2: Optimized Geometric H-Bond Parameters of the Lowest-Energy Conformation for the Four Diols

species	r_{O-H}/pm		$r_{H\cdots O}$	$\angle O-H\cdots O$	$r_{mid}{}^a$	$\theta_{OH\cdots OH}{}^b$
	OH_{free}	OH_{intra}	pm	deg	pm	deg
1,2-EG	96.8	97.2	238.5	106.4	295.7	61.2
1,2-PD	96.8	97.3	227.6	109.7	287.4	57.2
2,3-BD	96.9	97.3	217.9	111.8	279.3	53.6
1,2-BD	96.8	97.2	225.9	110.1	286.1	56.8

[a] Distance between the mid points of the two O−H bonds. [b] Angle between the two O−H bonds.

TABLE 3: Calculated IR Frequencies (ν, cm^{-1}), Obtained Local Mode Frequency (ν^0, cm^{-1}), and Vibrational Coupling Constant (β, cm^{-1})

species	ν_i	ν_i^0	$\nu_i^0 - \nu_i$	β
1,2-EG	3729.736	3729.755	0.019	0.9252
	3775.349	3775.330	−0.019	
1,2-PD	3716.442	3716.444	0.002	0.3747
	3774.590	3774.587	−0.003	
2,3-BD	3713.135	3713.136	0.001	0.2722
	3764.444	3764.442	−0.002	
1,2-BD	3719.482	3719.485	0.003	0.3877
	3774.295	3774.293	−0.002	

frequency difference gives $\Delta\nu_{CE} = 11.1$ cm^{-1} for 1,2-PD. Similarly, $\Delta\nu_{CE} = 9.7$ cm^{-1} is obtained for 1,2-BD from the FTIR spectra of 1-butanol and 2-butanol, whose free OH stretch frequencies are 3640.2 and 3630.5 cm^{-1}, respectively (data taken from NIST Chemistry WebBook[31]). We believe that these values are probably the most reasonable approximation one can make for the CE effect on OH groups in the four species.

Pairwise anharmonic vibrational coupling (β) between two of the OH stretching vibrators will cause a frequency separation ($\Delta\nu_{VC}$), which can be evaluated by decoupling the wave functions of the coupled normal modes.[32,33] This is a vibrational Hamiltonian-based approach. Briefly, in this approach, the degree of mode delocalization and vibrational coupling is encoded in their wave function mixing. The observed IR transition energies of the two OH groups are regarded to be a linear combination of local (uncoupled) OH stretching modes. The normal-mode eigenvectors can be used to decouple the two modes. For the two vibrator system, such a decoupling process is straightforward if the mode is assumed to be localized on the O−H stretching motion, which is the case here. With this approach, local-mode frequencies, vibrational coupling constant, and local-mode transition dipoles are obtained. The obtained coupling contains both through-bond (mechanical) and through-space (electrostatic) contributions. In this context, the gas-phase low-energy conformation of diols should be a reasonable starting point. Each of the conformations predicted by ab initio computations at the B3LYP/6-31+G* level possesses the five-membered quasi-ring structure (Figure 1 inserts). Table 2 lists optimized H-bonding geometric parameters for the four diols with the lowest energy conformation. In these conformations, the two OH groups are aligned in the same direction (with an acute angle), suggesting a positive transition dipolar coupling. In solution phase, the ring-structured conformation is also believed to be most stable for monodispersed diols in nonpolar solvent such as CCl$_4$. Therefore, we use these structures to evaluate the vibrational coupling effect on $\Delta\nu$ and IR intensity transfer.

Table 3 shows the calculated normal-mode (ν) and local mode frequencies (ν^0) and vibrational coupling constant (β) for the four diols. It is found that β is generally smaller than 1 cm^{-1},
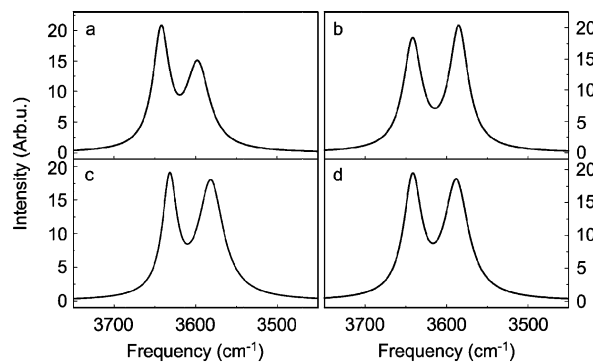
Figure 3. Calculated IR spectra of four diols with experimental broadenings and computed total intensities: (a) 1,2-EG, (b) 1,2-PD, (c) 2,3-BD, (d) 1,2-BD.

which is due to the highly localized nature of the OH stretching vibration. With such small β values and relatively larger frequency separations, $\Delta\nu_{VC}$ is expected to be small ($<2\beta$). Coupling-caused frequency separation reaches its maximum only when two local mode transition energies are degenerate, where one finds $\Delta\nu_{VC} = 2|\beta|$.

Because the IR intensity is proportional to the strength of the transition dipole, the effect of coupling on the intensity can be evaluated. For this, we still use the computed IR intensities from the four optimized structures. First, ab-initio-computations-yielded IR spectra in the OH stretch region are given in Figure 3. Here a frequency scaling factor (0.9647) is used. The computed IR transition frequencies are broadened according to experimentally obtained band widths with integrated areas equal to the computed transition intensities. As can be seen, after the scaling, the computed frequency separations are quite similar to the experimental values. However, the intensities of the two bands in each case are not always similar to experiments. This is because in the solution phase, there are also non-H-bonded species that contribute to the observed free OH stretching bands. Using the computed IR intensities, the ratio of the transition dipole strength between two normal modes is defined as $P = |\mu_{intra}|^2/|\mu_{free}|^2$, whereas that of the local modes is defined as $Q = |\mu_{intra}^0|^2/|\mu_{free}^0|^2$, and thus the ratio Q/P can be used to correct IR intensities. Here we use Q/P to scale the experimentally observed intensities to remove the coupling effect. If we assume that there are only two sources for the intensity transfer, namely, coupling and H-bonding, then the intensity ration purely due to H-bonding becomes $R_{HB} = (S_{intra}/S_{free})_{HB} = R \cdot Q/P$. Again, the above modelings are based on the gas-phase optimized structures, and the structural dependence of Q/P is ignored. The obtained transition dipole magnitudes and ratio of transition dipole strengths, experimentally observed ratio (R) for integrated peak area, and its correction factor, Q/P, as well as the corrected ratio, R_{HB}, are listed in Table 4.

Once $\Delta\nu_{CE}$ and $\Delta\nu_{VC}$ are available, the value of $\Delta\nu_{HB}$ in each case can be determined using eq 1. The values of all terms in the four cases are listed in Table 5. By removing the CE and VC effects, $\Delta\nu_{HB}$ is found to be generally smaller than $\Delta\nu$ in all cases and significantly smaller for the asymmetric diols.

H-Bonding Caused Infrared Intensification. As has been shown above (Table 4), the HB enhancement of the transition intensity, that is, R_{HB}, can be obtained by removing the VC effect from the observed R value. This is done by using the vibrational coupling, transition dipole, and OH bond angle of the low-energy conformation in each case. It has been found[34] that the anharmonic properties of the fundamental and overtone transitions of an acceptor OH in vicinal diols are not significantly

Subtle Variation of Weak IHB in Vicinal Diols

J. Phys. Chem. A, Vol. 113, No. 21, 2009 **6073**

TABLE 4: Calculated Normal-Mode Transition Dipole Moment (μ, D), Ratio of the Transition Dipole Strength ($P = |\mu_{intra}|^2/|\mu_{free}|^2$), Local-Mode Transition Dipole Moment (μ^0, D), Ratio of the Local-Mode Transition Dipole Strength ($Q = |\mu_{intra}^0|^2/|\mu_{free}^0|^2$), Ratio Q/P, Experimentally Observed Peak Area Ratio (R), and That Due to H-Bond Only (R_{HB}) for the Four Diols

species	μ	P	μ^0	Q	Q/P	R	R_{HB}
1,2-EG	0.0623	1.02286	0.0633	1.08393	1.0597	1.18	1.25
	0.0616		0.0608				
1,2-PD	0.0666	1.17273	0.0669	1.19886	1.0223	1.01	1.03
	0.0615		0.0611				
2,3-BD	0.0710	1.76120	0.0713	1.79620	1.0199	1.79	1.83
	0.0535		0.0532				
1,2-BD	0.0706	1.33514	0.0710	1.37269	1.0281	1.16	1.19
	0.0611		0.0606				

affected by H-bonding, justifying its usage as the "free" OH group. The obtained R_{HB} values are listed in Table 4. It is found that the value of R_{HB} is 2−6% larger than that of R, and exhibits a quantitative linear relationship with $\Delta\nu_{HB}$

$$R_{HB} = 0.04663\Delta\nu_{HB} - 0.2665 \quad (2)$$

A plot of R_{HB} versus $\Delta\nu_{HB}$ is shown in Figure 4 (top, dots). The correlation coefficient between R_{HB} and $\Delta\nu_{HB}$ is found to be 0.99. Equation 2 means the larger the $\Delta\nu_{HB}$, the larger the R_{HB}. Therefore, we believe that R_{HB} can probably serve as a measure of the HB strength in these molecules. In general, forming an IHB will lengthen the O−H equilibrium distance and increase the magnitude of the electric transition dipole moment of the mode,[6] which is the origin of the intensity enhancement of the OH$_{intra}$ band. Furthermore, the found linear relationship between $\Delta\nu_{HB}$ and R_{HB} shown above suggests that the obtained $\Delta\nu_{HB}$ is proportional to the amount of such intensity enhancement. Therefore, $\Delta\nu_{HB}$ reflects the intrinsic property of the changed vibrational potential surface due to the IHB. Here the CE effect on R is assumed to be very small and thus neglected. However, according to Scheme 1, there are two parts of free OH on the right side and one part of "free" OH on the left side. They must have overlapping stretching frequencies because experimentally, only two OH stretching bands are observed. Therefore it has to be pointed out that R_{HB} is only an apparent measure of H-bonding resulted enhancement. The actual intensification of the H-bonded OH stretching band should be a few percent larger than R_{HB} (related to the equilibrium constant K, see below). The interplay of CE, VC, and HB on the frequency and intensity of the two OH modes for vicinal diols is illustrated in Figure 4 (bottom).
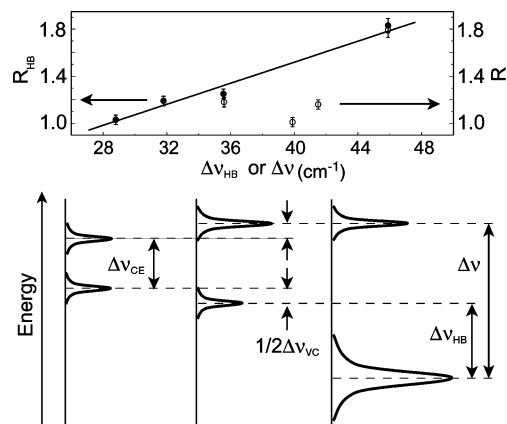
Enthalpies of Intramolecular Hydrogen Bond Formation. The enthalpies can be estimated on the basis of experimental and computational results. First, the vibrational contribution to the O···H−O IHB formation enthalpy, denoted as ΔH_{HB}^V, can be computed using $\Delta H_{HB}^V = h\Delta\nu_{HB}$,[6] which is a direct vibrational energy drop upon forming the IHB. Here h is Planck's constant.

Figure 4. Linear relationship between IHB-resulted integrated area ratio R_{HB} and $\Delta\nu_{HB}$ (●) and plot of observed ratio R and $\Delta\nu$ (○) (top). Illustration of OH stretching transition energy separation and intensity change due to hydrogen bonding, vibrational coupling, and chemical environment effect in diol (bottom).

The results are given in Table 5. Then, the total IHB formation enthalpy, ΔH, can be estimated (Table 5). On the basis of Scheme 1, a relationship between R_{HB} and the equilibrium constant, K, can be found: $R_{HB} = Q/(1 + 2K)$, so that $K = (Q/R_{HB} - 1)/2$. Using $RT \ln K = -\Delta H + T\Delta S$ and ignoring $T\Delta S$ at room temperature, we can estimate ΔH. We find $K = 0.082$ and $\Delta H = -1.48$ kcal/mol for 1,2-PD and, $K = 0.077$ and $\Delta H = -1.52$ kcal/mol for 1,2-BD. However, such an attempt for 1,2-EG and 2,3-BD is impractical because in these two cases, the Q values are smaller than the R_{HB} values.
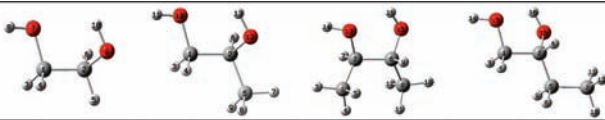
The total HB formation enthalpy can also be estimated using the empirical equations. According to recent studies,[21,26] the transition frequencies and their separation of H-bond-forming species are connected to the enthalpy of the H-bond formation by the B−B equation[23,24]

$$\Delta\nu/\nu = -k\Delta H^{BB} \quad (3)$$

here $\Delta\nu$ is the total frequency separation between free and H-bonded OH stretching modes, ν is the frequency of the free OH stretching mode, and $k = 1.7 \times 10^{-2}$ mol/kcal is a constant.[35] The estimated values of the four diols using eq 3 are listed in Table 5. The total IHB formation enthalpies can also be evaluated using Iogansen's equation[25]

$$\Delta H^I = -0.3312(\Delta\nu - 40)^{1/2} \quad (4)$$

with ΔH^I in kilocalories per mole. Even though this equation does not apply to the case in which $\Delta\nu \leq 40$ cm^{-1},[25] the estimated values of 2,3-BD and 1,2-BD are very close to those from the B−B equation. However, it seems that both the empirical equations yield underestimated enthalpies, suggesting that these empirical eqs 3 and 4 may not be applicable to intramolecular H-bonding situations.

TABLE 5: Contributions to the OH Stretch Frequency Separation (cm^{-1}), HB Enhancement (R_{HB}), and Vibrational Contribution to the HO···HO H-Bond Formation Enthalpy (ΔH_{HB}^V, ΔH, ΔH_{BB} and ΔH^I in kcal/mol) for the Four Diols

species	$\Delta\nu$	$\Delta\nu_{CE}$	$\Delta\nu_{VC}$	$\Delta\nu_{HB}$	R_{HB}	$\Delta H_{HB}^{V\ a}$	ΔH^b	ΔH_{BB}^c	ΔH^{Id}
1,2-EG	35.6	0.0	0.04	35.56	1.25	−0.1017		−0.5749	
1,2-PD	39.9	11.1	0.01	28.79	1.03	−0.0824	−1.4811	−0.6453	
2,3-BD	45.9	0.0	0.00	45.90	1.83	−0.1313		−0.7426	−0.8045
1,2-BD	41.5	9.7	0.01	31.79	1.19	−0.0909	−1.5200	−0.6708	−0.4056

^{a} Obtained using $\Delta H_{HB}^V = h\Delta\nu_{HB}$.[6] ^{b} $\Delta H = -RT \ln K$. ^{c} Obtained using the B−B relationship[21,26] based on $\Delta\nu$. ^{d} Obtained using the Iogansen equation[25] based on $\Delta\nu$.

TABLE 6: NPA Charges (in e) for the Four Diols

C 1	-0.14820	C 1	-0.13467	C 1	-0.70763	C 1	-0.13354
C 2	-0.13680	C 2	0.03744	C 2	0.03746	C 2	0.04963
H 3	0.20759	H 3	0.20821	H 3	0.23680	H 3	0.20735
H 4	0.20909	H 4	0.20696	H 4	0.24323	H 4	0.20855
H 5	0.22893	C 5	-0.69786	H 5	0.24359	C 5	-0.48441
H 6	0.20856	H 6	0.21635	C 6	0.05139	H 6	0.21334
O 7	-0.79582	H 7	0.25381	H 7	0.21564	C 7	-0.68900
H 8	0.50227	H 8	0.24000	C 8	-0.69733	H 8	0.23690
O 9	-0.77897	H 9	0.23704	H 9	0.21382	H 9	0.24129
H10	0.50337	O10	-0.79395	H10	0.25555	H10	0.23570
		H11	0.50278	H11	0.23567	H11	0.25239
		O12	-0.78395	H12	0.23858	H12	0.23008
		H13	0.50784	O13	-0.79415	O13	-0.79353
				H14	0.50087	H14	0.50276
				O15	-0.78430	O15	-0.78664
				H16	0.51080	H16	0.50912

In an intermediate-strength HB system, the enthalpy is about -5 to -10 kcal/mol, out of which one tenth comes from vibration.[6] The results in Table 5 suggest that IHB in the diols is in the weak HB regime. Take 1,2-BD as an example: ΔH_{HB}^V accounts for roughly 1/16 of the total HB interaction energy, ΔH. Nevertheless, on the basis of $\Delta \nu_{HB}$ and ΔH_{HB}^V, we conclude that the vibrational contributions to the total ΔH are ordered as 2,3-BD > 1,2-EG > 1,2-BD > 1,2-PD. In other words, 1,2-PD has the smallest vibrational stabilization for the IHB. Furthermore, the values ΔH^{BB} also suggest that 1,2-PD has the weakest IHB among the four molecules.

Nature of Intramolecular Hydrogen Bond in Diols. Relative strengths of the H-bonds in the diols are shown in their bond length and angle between two OH bonds in each case. The O−H bond length and H-bonding parameters listed in Table 2 clearly show that the shortest HB donor−acceptor distance (H···O) is observed in 2,3-BD ($r_{H\cdots O} = 217.9$ pm), whereas the OH bond length is the longest ($r_{O-H} = 97.3$ pm), suggesting a relatively stable intramolecular H-bond.

The NPA[29] is used to examine the H-bond-induced charge redistributions. The results are listed in Table 6. It is seen that C1 and C2 atoms in 1,2-EG have different charges as a result of forming the intramolecular H-bond. Similarly, it is seen that in 2,3-BD, C2 and C6 atoms have different charges, and even C1 and C8 in two methyl groups have different charges, suggesting that the two methyl groups are affected by the IHB: the two groups seem to be involved differently (electron pushing versus pulling) in the formation of the H-bonded complex.

The intrinsic nature of HB has been believed to be a subtle balance of hyperconjugation and rehybridization effects.[36] NBO[30] computations show that all four diols have hyperconjugative interactions between the HB acceptor oxygen lone-pair orbital $n(O)$ and the HB donor O−H σ antibond orbital $\sigma^*(O-H)$ (Table 7), suggesting the presence of an IHB.[18] The

hyperconjugation will lengthen the donor O−H bond length, leading to a red shift of the donor O−H stretch frequency. Even though the predicted order of the hyperconjugation interaction for the four diols is not the same as that of the obtained $\Delta \nu_{HB}$, the computations show that 2,3-BD has the most significant hyperconjugative interaction between $n(O)$ and $\sigma^*(O-H)$ orbitals, suggesting the presence of the strongest IHB among the four molecules. On the contrary, when the rehybridization dominates, as occurred in the case of the C−H···X complex, the C-hybrid orbital in the C−H bond undergoes a significant change in hybridization and polarization,[36] and a blue shift of the C−H stretch frequency shall be observed, which is beyond the scope of the present work.

The difference of the IHB situations in these diols is actually revealed by their IR absorption line widths from the dynamics aspect. For example, as seen in Table 1, for 2,3-BD, $\nu_{1/2}$ of OH_{free} is the narrowest and that of OH_{intra} is the broadest, which is consistent with the picture that a relatively stronger HB is formed between the two OH groups. Because of the same reason, more inhomogeneous broadening is seen in the bandwidth of the latter than in the former. The structurally dependent IR line width may be understood on the basis of the size of chemical groups in the neighborhood and their roles in affecting the IHB stability. In a small flexible system such as 1,2-EG, every atom moves dynamically, and thus it is not expected to form a very stable IHB. In 2,3-BD, two methyl groups exhibit different charge distributions associated with the formed IHB, as seen from NPA shown in Table 6. One may argue the other way around that the different charge distribution may promote the formation of the IHB, as discussed previously in the formation of an intermolecular HB by dimethyl sulfoxide/methanol complex.[37] For 1,2-BD, the larger size of the alkyl group on one side may promote the separation of the hydrophobic and hydrophilic terminus of the molecule and thus indirectly stabilize the IHB. The least stable IHB in 1,2-PD might have something to do with both the size of the alkyl groups and the asymmetric structure of itself.

Furthermore, the temperature-dependent linear IR experiment (Figure 5) also suggests the presence of IHB in each case. Figure 5 shows FTIR spectra of the four diols at 80 °C in comparison with those at 23 °C. Spectral fitted parameters and estimated ratios of the integrated area for the 80 °C spectra are given in Table 8. It is found that the values of ν and $\nu_{1/2}$ of the two OH absorption bands change to different extents as a function of temperature for the four diols. In particular, $\Delta \nu$ and R values at higher temperature (80 °C) are found to be somewhat smaller than those at room temperature, showing the signature of breaking the IHB as temperature increases. In addition, the temperature-dependent linear IR measurements can be used to compute the enthalpies of forming IHB for the four diols.[10,38,39] However, this requires a careful experimental determination of the absorption coefficient for the free and H-bonded OH stretching bands. Because there are only two OH bands in this region but the equilibrium shown in Scheme 1 involves three

TABLE 7: NBO Analysis for the Four Diols[a]

species	entity	energy of bonds and lone pairs	important admixtures: entity and (stabilization)
1,2-EG	O7 π lone pair	-0.33032	C1C2* (0.55), C1H4* (2.92), C1H3* (7.30), **O9H10* (0.82)**
1,2-PD	O10 π lone pair	-0.34013	C1C2* (0.70), C1H3* (7.19), C1H4* (2.47), **O12H13* (1.42)**
2,3-BD	O13 π lone pair	-0.33644	C2H7* (2.56), C1C2* (6.86), C1H4* (0.96), **O15H16* (2.04)**
1,2-BD	O13 π lone pair	-0.34090	C1C2* (0.71), C1H3* (2.39), C1H4* (7.16), **O15H16* (1.53)**

[a] Energy of NBO entities are reported in hartree. The stabilizations are in kilocalories per mol. Interactions of "geminal" entities (sharing a common atom) and those less than 0.5 kcal/mol are not reported.

Subtle Variation of Weak IHB in Vicinal Diols

J. Phys. Chem. A, Vol. 113, No. 21, 2009 **6075**
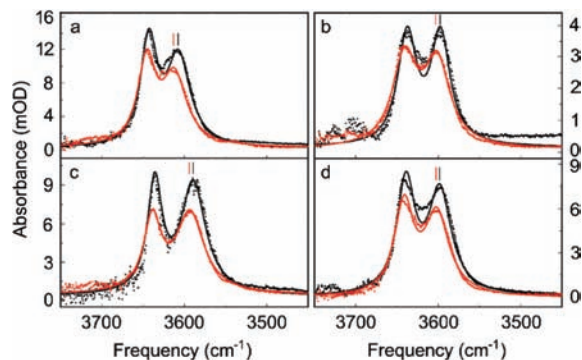
Figure 5. FTIR spectra of the four diols in CCl$_4$ in the OH stretching region at 23 °C (black) and 80 °C (red): (a) 1,2-EG, (b) 1,2-PD, (c) 2,3-BD, and (d) 1,2-BD. Noisy signals at the higher frequency end are due to residue water in the sample. Fitting uses Lorentzian function. Two vertical bars indicate the blue shift of the OH$_{intra}$ band from 23 to 80 °C.

TABLE 8: Frequency (ν, cm^{-1}), Full Width at Half-Maximum ($\nu_{1/2}$, cm^{-1}), Frequency Shift ($\Delta\nu$, cm^{-1}), and Integrated Peak Area Ratio (R) of the Two OH Absorption Bands for the Four Diols Obtained at 80 °C

species	OH$_{free}$		OH$_{intra}$		$\Delta\nu$	R
	ν	$\nu_{1/2}$	ν	$\nu_{1/2}$		
1,2-EG	3645.6	26.0	3612.0	36.1	33.6	1.16
1,2-PD	3640.9	35.8	3601.7	37.8	39.2	1.01
2,3-BD	3638.6	25.6	3593.0	40.1	45.6	1.77
1,2-BD	3641.3	28.4	3601.4	36.2	39.9	1.15

parts of free OH and one part of H-bonded OH, experimentally measuring the total enthalpy remains to be a difficult case at the moment. However, as we have shown above, the equilibrium constant, K, and enthalpy, ΔH, can be roughly estimated on the basis of room-temperature linear IR results and ab initio computations.

Concluding Remarks

In summary, by taking linear IR measurements in the OH stretching region, by performing ab initio quantum chemical computations on transition frequency and transition dipole, and by using vibrational excitonic Hamiltonian modeling, the present study reveals the physical basis of the observed total IR frequency shift of the two OH stretching bands and the IR intensifications of the H-bonded OH band in vicinal alkyl diols. The dissection of the total frequency shift by eq 1 has been successfully demonstrated. Using the obtained $\Delta\nu_{HB}$ as a measure, the vibrational stabilization contributions to the enthalpy of the IHB formation for the four vicinal diols are determined. The enthalpies of IHB formations in these diols are estimated by several methods, including two empirical equations. These results are used to differentiate the HB strength in these similar IHB complexes. The formed IHB is found to be in the weak H-bond regime for the four diols. Our results suggest that 1,2-PD has the weakest IHB and 1,2-BD has the strongest IHB among the four diol molecules. A linear relationship between the "purely" H-bond-induced frequency separation and the corrected peak enhancement is found.

A general approach to decoupling the IR transition frequency and transition intensity of highly localized modes together is proposed. The uncoupled local mode frequencies and their IR intensities can be easily obtained. We find that the computations and modelings can become very useful in interpreting experimental results. The approach outlined here may be applied to

diols with cyclic chains and even to IHB systems involving other functional groups such as N–H in peptides and nucleic acids.

Even though we present a case study of four linear diols, one may speculate that the obtained $\Delta\nu_{HB}$ may be a true measure of vibrational intensity enhancement because of the IHB complex formation for any vicinal diols with even bigger R_1 and R_2 alkyl groups (Scheme 1). Furthermore, $\Delta\nu_{HB}$ shall work better than R_{HB} in the case where more than one species are involved and have overlapping IR absorption bands, as shown in the diols present here. On the basis of these considerations, a general caution should be taken when using the observed frequency shift to evaluate the strength of a HB directly because $\Delta\nu$ is usually not the same as $\Delta\nu_{HB}$. Furthermore, it should be pointed out that the anharmonic vibrational coupling resultant frequency shift is found to be negligibly small in the case of OH stretch modes; however, this may not be the case in other systems such as the C=O stretch modes in peptides. Recent studies showed that vibrational coupling in the latter case can easily be of a few cm^{-1} and is thus non-negligible.[33]

The results from this study shall be helpful in understanding the origins of changes in both the frequency and line shape of the OH stretching band. The chemical environment, vibrational coupling, and H-bonding condition, all play a certain role in this regard. It is these factors that determine the local structural sensitivity of the OH mode. The OH mode can be used as vibrational spectroscopic probes for local structures and dynamics of H-bonded molecular systems in condensed phases, as has been recently explored by nonlinear IR techniques.[40–42]

References and Notes

(1) Jeffrey, G. A. *An Introduction to Hydrogen Bonding*; Oxford University Press: New York, 1997.

(2) Ballisent-Funel, M.-C.; Dore, J. C. *Hydrogen Bond Networks*; Kluwer Academic Publisher: Dordecht, The Netherlands, 1993.

(3) Foti, M. C.; Barclay, L. R. C.; Ingold, K. U. *J. Am. Chem. Soc.* **2002**, *124*, 12881–12888.

(4) Clarkson, J. R.; Baquero, E.; Shubert, V. A.; Myshakin, E. M.; Jordan, K. D.; Zwier, T. S. *Science* **2005**, *307*, 1443–1446.

(5) Tian, S. X.; Yang, J. *Angew. Chem., Int. Ed.* **2006**, *118*, 2123–2126.

(6) Maréchal, Y. *The Hydrogen Bond and the Water Molecule: The Physics and Chemistry of Water, Aqueous, and Bio Media*; Elsevier: Amsterdam, 2007.

(7) Markle, T. F.; Mayer, J. M. *Angew. Chem., Int. Ed.* **2008**, *120*, 750–752.

(8) Gallwey, F. B.; Hawkes, J. E.; Haycock, P.; Lewis, D. *J. Chem. Soc., Perkin Trans. 2* **1990**, *11*, 1979–1985.

(9) Wang, F.; Polavarapu, P. L. *J. Phys. Chem. A* **2001**, *105*, 6991–6997.

(10) Fishman, E.; Chen, T. L. *Spectrochim. Acta, Part A* **1969**, *25*, 1231–1242.

(11) Singelenberg, F. A. J.; Van Der Maas, J. H. *J. Mol. Struct.* **1991**, *243*, 111–122.

(12) Yamamoto, K.; Nakao, Y.; Kyogoku, Y.; Sugeta, H. *J. Mol. Struct.* **1991**, *242*, 75–86.

(13) Crupi, V.; Maisano, G.; Majolino, D.; Migliardo, P.; Venuti, V. *J. Phys. Chem. A* **2000**, *104*, 3933–3939.

(14) Jesus, A. J. L.; Rosado, M. T. S.; Leitao, M. L. P.; Redinha, J. S. *J. Phys. Chem. A* **2003**, *107*, 3891–3897.

(15) Nagy, P. I.; Dunn, W. J.; Alagona, G.; Ghio, C. *J. Am. Chem. Soc.* **1992**, *114*, 4752–4758.

(16) Manivet, P.; Masella, M. *Chem. Phys. Lett.* **1998**, *288*, 642–646.

(17) Foti, M. C.; DiLabio, G. A.; Ingold, K. U. *J. Am. Chem. Soc.* **2003**, *125*, 14642–14647.

(18) Trindle, C.; Crum, P.; Douglass, K. *J. Phys. Chem. A* **2003**, *107*, 6236–6242.

(19) Crittenden, D. L.; Thompson, K. C.; Jordan, M. J. T. *J. Phys. Chem. A* **2005**, *109*, 2971–2977.

(20) Klein, R. A. *J. Am. Chem. Soc.* **2002**, *124*, 13931–13937.

(21) Klein, R. A. *J. Comput. Chem.* **2003**, *24*, 1120–1131.

(22) Klein, R. A. *Chem. Phys. Lett.* **2006**, *429*, 633–637.

(23) Badger, R. M.; Bauer, S. H. *J. Chem. Phys.* **1937**, *5*, 839–851.

(24) Badger, R. M. *J. Chem. Phys.* **1940**, *8*, 288–289.

(25) Iogansen, A. V. *Spectrochim. Acta, Part A* **1999**, *55*, 1585.

(26) Bangal, P. R.; Chakravorti, S. *J. Phys. Chem. A* **1999**, *103*, 8585–8594.

(27) Jesus, A. J. L.; Rosado, M. T. S.; Reva, I.; Fausto, R.; Eusébio, M. E.; Redinha, J. S. *J. Phys. Chem. A* **2006**, *110*, 4169–4179.

(28) Watson, T. M.; Hirst, J. D. *J. Phys. Chem. A* **2002**, *106*, 7858–7867.

(29) Carpenter, J. E.; Weinhold, F. *J. Mol. Struct. (THEOCHEM)* **1988**, *169*, 41–62.

(30) Frisch, M. J.; Trucks, G. W.; Schlegel, H. B.; Scuseria, G. E.; Robb, M. A.; Cheeseman, J. R.; Montgomery, J. A., Jr.; Vreven, T.; Kudin, K. N.; Burant, J. C.; Millam, J. M.; Iyengar, S. S.; Tomasi, J.; Barone, V.; Mennucci, B.; Cossi, M.; Scalmani, G.; Rega, N.; Petersson, G. A.; Nakatsuji, H.; Hada, M.; Ehara, M.; Toyota, K.; Fukuda, R.; Hasegawa, J.; Ishida, M.; Nakajima, T.; Honda, Y.; Kitao, O.; Nakai, H.; Klene, M.; Li, X.; Knox, J. E.; Hratchian, H. P.; Cross, J. B.; Bakken, V.; Adamo, C.; Jaramillo, J.; Gomperts, R.; Stratmann, R. E.; Yazyev, O.; Austin, A. J.; Cammi, R.; Pomelli, C.; Ochterski, J. W.; Ayala, P. Y.; Morokuma, K.; Voth, G. A.; Salvador, P.; Dannenberg, J. J.; Zakrzewski, V. G.; Dapprich, S.; Daniels, A. D.; Strain, M. C.; Farkas, O.; Malick, D. K.; Rabuck, A. D.; Raghavachari, K.; Foresman, J. B.; Ortiz, J. V.; Cui, Q.; Baboul, A. G.; Clifford, S.; Cioslowski, J.; Stefanov, B. B.; Liu, G.; Liashenko, A.; Piskorz, P.; Komaromi, I.; Martin, R. L.; Fox, D. J.; Keith, T.; Al-Laham, M. A.; Peng, C. Y.; Nanayakkara, A.; Challacombe, M.; Gill, P. M. W.; Johnson, B.; Chen, W.; Wong, M. W.; Gonzalez, C.; Pople, J. A. Gaussian 03, revision B05; Gaussian, Inc.: Wallingford, CT, 2004.

(31) *NIST Chemistry WebBook*; NIST Standard Reference Database Number 69; National Institute of Standards and Technology: Gaithersburg, MD.

(32) Wang, J.; Hochstrasser, R. M. *J. Phys. Chem. B* **2006**, *110*, 3798–3807.

(33) Wang, J.; Hochstrasser, R. M. *Chem. Phys.* **2004**, *297*, 195–219.

(34) Iwamoto, R.; Matsuda, T.; Kusanagi, H. *Spectrochim. Acta, Part A* **2005**, *62*, 97–104.

(35) Zadorozhnyi, B. A.; Ishchenko, I. K. *Opt. Spectrosc.* **1965**, *19*, 306.

(36) Alabugin, I. V.; Manoharan, M.; Peabody, S.; Weinhold, F. *J. Am. Chem. Soc.* **2003**, *125*, 5973–5987.

(37) Li, Q.; Wu, G.; Yu, Z. *J. Am. Chem. Soc.* **2006**, *128*, 1438–1339.

(38) Lin, T.-S.; Fishman, E. *Spectrochim. Acta, Part A* **1967**, *23*, 491–500.

(39) Baker, A. W.; Shulgin, A. T. *Can. J. Chem.* **1965**, *43*, 650−659.

(40) Nibbering, E. T. J.; Elsaesser, T. *Chem. Rev.* **2004**, *104*, 1887–1914.

(41) Lock, A. J.; Gilijamse, J. J.; Woutersen, S.; Bakker, H. J. *J. Chem. Phys.* **2004**, *120*, 2351–2358.

(42) Kuo, C.-H.; Vorobyev, D. Y.; Chen, J.; Hochstrasser, R. M. *J. Phys. Chem. B* **2007**, *111*, 14028–14033.